Rare earth Ce-modified (Ti,Ce)/a-C:H carbon-based film on WC cemented carbide substrate*

Shengguo Zhou(周升国)[1,†], Zhengbing Liu(刘正兵)[1], and Shuncai Wang(王顺才)[2]

[1] School of Material Science and Engineering, Jiangxi University of Science and Technology, Ganzhou 341000, China
[2] National Centre for Advanced Tribology at Southampton, School of Engineering Sciences, University of Southampton, Southampton, UK

(Received 16 September 2016; revised manuscript received 6 October 2016; published online 10 December 2016)

WC cemented carbide suffers severe wear in water environments. A novel carbon-based film could be a feasible way to overcome this drawback. In this study, a rare earth Ce-modified (Ti,Ce)/a-C:H carbon-based film is successfully prepared on WC cemented carbide using a DC reactive magnetron sputtering process. The microstructure, mechanical properties, and tribological behavior of the as-prepared carbon-based film are systematically investigated. The results show that the doping Ti forms TiC nanocrystallites that are uniformly dispersed in the amorphous carbon matrix, whereas the doping Ce forms CeO_2 that exists with the amorphous phase in the co-doped (Ti,Ce)/a-C:H carbon-based film. The mechanical properties of this (Ti,Ce)/a-C:H film exhibit remarkable improvements, which could suggest higher hardness and elastic modulus as well as better adhesive strength compared to solitary Ti-doped Ti/a-C:H film. In particular, the as-prepared (Ti,Ce)/a-C:H film presents a relatively low friction coefficient and wear rate in both ambient air and deionized water, indicating that (Ti,Ce)/a-C:H film could feasibly improve the tribological performance of WC cemented carbide in a water environment.

Keywords: rare earth, (Ti,Ce)/a-C:H, cemented carbide, tribological

PACS: 81.05.U–, 68.55.–a, 81.15.Cd, 81.40.Pq **DOI:** 10.1088/1674-1056/26/1/018101

1. Introduction

WC cemented carbide offers high strength, high hardness, high temperature resistance, oxidation resistance, and chemical corrosion resistance, and is widely used in petroleum drilling, mechanical seals, underwater strand pelletizing systems, underwater axle bearings, and so on.[1–4] Unfortunately, when WC cemented carbide is used in water environments, it exhibits poor tribological performance because of the low viscosity of water. In particular, it offers less lubrication, causing the friction coefficient to rise sharply and resulting in very serious wear under conditions in which the friction pair suffers instantaneous overload or frequent start–stop phases.[5,6] Therefore, enhancing the surface of WC cemented carbide so as to eliminate these problems in water environments is of significant importance. Diamond-like carbon (DLC) films possess high hardness, low friction, and high wear resistance. Thus, they have widespread applications in many industrial fields, and could exhibit good tribological performance in water environments.[7–13] As a result, it should be feasible to deposit DLC films on WC cemented carbide to achieve better tribological performance.

The relatively high internal stress and low toughness of DLC could cause low adhesion and even peeling of the films from substrates. It has been reported that a metallic Ti transition layer enhances the adhesion strength to the substrate; metallic Ti doping could also reduce internal stress significantly while maintaining the hardness, friction coefficient, and wear of DLC films.[13–15] In particular, it was reported that co-doping in DLC films could improve their tribological performance, e.g., aluminum/titanium, aluminum/chromium, copper/titanium co-doped DLC films.[16–18] DLC doping with rare earth elements is an important direction of research in surface engineering. The resulting DLC films could exhibit good internal stress, friction coefficient, and wear rate properties.[19,20] When a rare earth element was used to dope DLC film, the internal stress decreased by approximately 70% and the friction coefficient went from 0.1 to 0.09.[20] Moreover, the doped rare earth element was dissolved within the DLC amorphous matrix, but did not form nanoparticles.[21,22] Although duplex-doped DLC film with rare earth elements has been reported, this combined a single rare earth element with another element, such as cerium and lanthanum.[19,23] There are few reports of rare earth elements accompanied by metallic titanium to prepare duplex-doped nanocomposite carbon-based film. Additionally, this rare earth modified carbon-based film does not appear to have been used as a strategy to improve WC cemented carbide.

In this paper, we report the use of Ce-modified nc-TiC/a-C:H carbon-based film to prepare (Ti,Ce)/a-C:H composite carbon-based film on a WC cemented carbide substrate using a DC reactive magnetron sputtering process. The morphologies, microstructure, and mechanical properties of the as-prepared

*Project supported by the National Natural Science Foundation of China (Grant Nos. 51302116 and 51365016) and the Program for Excellent Young Talents, Jiangxi University of Science and Technology, China.

†Corresponding author. E-mail: zhoucreed@163.com,zhousg@jxust.edu.cn

(Ti,Ce)/a-C:H carbon-based film are systematically characterized, and the friction and wear behavior are evaluated in both ambient air and deionized water conditions.

2. Experimental procedure

The hydrogenated (Ti,Ce)/a-C:H carbon-based film was deposited on mirror-polished Si p(100) wafers and WC cemented carbide (Co% = 8 at.%) substrates (with dimensions of 30 mm × 30 mm × 2 mm) by DC reactive magnetron sputtering using CH_4 as the carbon source gas. To compare with (Ti,Ce)/a-C:H film, a solitary Ti-doped Ti/a-C:H was prepared simultaneously. It has been reported that the Co phase could induce interfacial graphitization and decrease the adhesion strength;[24] thus, pretreated WC cemented carbide using potassium hydroxide solution and Caro's acid were used to eliminate the Co phase from the WC cemented carbide substrate surface. Prior to deposition, the WC cemented carbide substrates were ultrasonically cleaned in acetone for 20 min, ethanol for 20 min, deionized water for 10 min, potassium hydroxide solution (10 g KOH + 100 ml H_2O) for 30 min, Caro's acid (30 ml H_2SO_4:70 ml H_2O_2) for 1 min, and deionized water for 10 min in succession, and then dried in nitrogen. As the pressure of the vacuum chamber reached the base pressure of 2.0×10^{-3} Pa, the pure Ti interlayer was deposited by two Ti targets (purity > 99.99 wt.%) so as to improve the adhesion strength. The deposition parameters of the Ti interlayer were as follows: temperature of 200 °C, pressure of 3 Pa, sputtering power of 200 W, Ar flow rate of 60 sccm, and deposition time of 15 min. On top of the Ti interlayer, carbon-based films were deposited using two targets in a CH_4 and Ar mixing gas atmosphere. Two Ti targets were used for the Ti/a-C:H film, and one Ti target and one Ti/Ce composite target (Ti concentration of 90 at.%) were used for the (Ti,Ce)/a-C:H film. A DC bias was applied to the substrates during deposition. The deposition parameters of the carbon based films are listed in Table 1.

Table 1. Deposition parameter of as-prepared carbon-based films.

Films	Pressure /Pa	Ar flow rate/sccm	CH_4 flow rate/sccm	Ti target sputtering power/W	Ti/Ce target sputtering power/W	Temperature /°C	Sputtering time/min
Ti/a-C:H	2.0	50	14	160	/	100	90
(Ti,Ce)/a-C:H	2.0	50	16	160	160	100	90

The as-prepared film thicknesses were measured by field emission scanning electron microscope (FESEM) (Hitachi S4800) via observation of their cross-sectional surface. The surface roughness and morphology were measured by atomic force microscopy (AFM) (CSPM5000). The chemical bonding states and composition of the as-prepared carbon-based films were confirmed by x-ray photoelectron spectroscopy (XPS) (Kratos AXIS ULTRA). The phases of the as-prepared films were characterized by x-ray diffraction (XRD) (Bruker D8 x-ray facility). The adhesion strength and hardness of the as-prepared films were evaluated using a Revetest CSM scratch tester and MTS Nano-Indenter G200 system. The tribological behavior of the Ti/a-C:H and (Ti,Ce)/a-C:H films in ambient air and deionized water conditions at room temperature were evaluated on the HSR-2M reciprocating sliding tribometer. As the counter body, the diameter of the WC cemented carbide ball was 5 mm, and all frictional tests were carried out under a load of 5 N, reciprocating frequency of 5 Hz, and an amplitude of 5 mm. Subsequently, the morphologies of the wear tracks and wear scars were characterized using a scanning electron microscope (SEM) (TM3030). The wear rates obtained after the sliding tests were completed based on the wear track depth profiles detected by a NanoMap 500LS profilometer.

3. Results and discussion

3.1. Composition and microstructure

The surface morphologies of the as-prepared Ti/a-C:H and (Ti,Ce)/a-C:H carbon-based films were characterized by AFM, as shown in Figs. 1(a) and 1(b) for the two- and three-dimensional surfaces, respectively. These morphologies indicate that the surface of the Ti/a-C:H and (Ti,Ce)/a-C:H films have a nanoscale concave–convex body, with the rare earth Ce-modified (Ti,Ce)/a-C:H carbon-based film exhibiting slightly more roughness than the Ti/a-C:H film. The average roughness of the Ti/a-C:H and (Ti,Ce)/a-C:H films were calculated to be approximately 1.15 nm and 1.32 nm (RMS), respectively. This variation can be attributed to the greater atomic mass of rare earth Ce compared with metallic Ti.

Cross-sections of the as-prepared Ti/a-C:H and (Ti,Ce)/a-C:H carbon-based films were characterized via FESEM, as shown in Fig. 2. From these images, the final thickness of the as-prepared carbon-based films can be measured as 0.89 μm for the Ti/a-C:H film and 0.92 μm for the (Ti,Ce)/a-C:H film. Thus, there is a small difference in the thickness of Ti/a-C:H and (Ti,Ce)/a-C:H carbon-based films. Because the rare earth Ce atoms are easier to ionize and sputter, the sputtered Ce ions or atoms have more possibility of being deposited on the substrate[19] when the sputtering power of the targets is the same and the electric field between the target and substrate

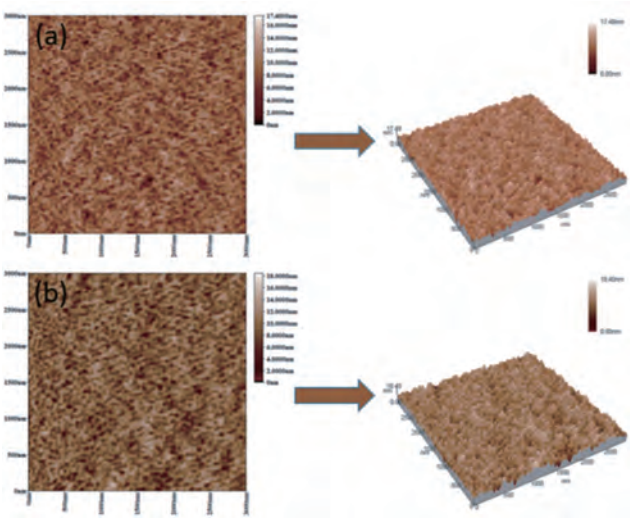

Fig. 1. (color online) The two- and three-dimensional AFM surface morphologies of (a) Ti/a-C:H film and (b) (Ti,Ce)/a-C:H film.

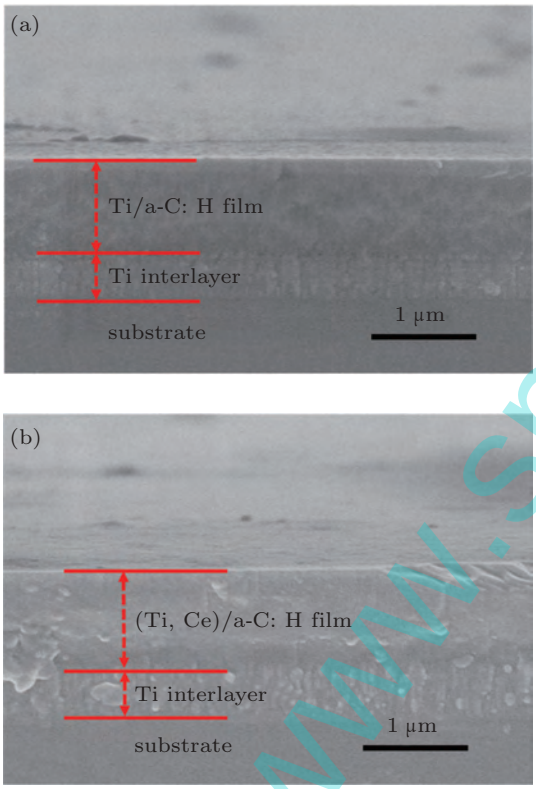

Fig. 2. (color online) Cross-sectional images of as-fabricated films: (a) Ti/a-C:H film and (b) (Ti,Ce)/a-C:H film.

is nearly the same. Additionally, the higher CH_4 flow rate (16 sccm) would lead to an increase in the thickness of the (Ti,Ce)/a-C:H carbon-based film. The cross-sectional morphologies suggest that the interlayer between the top-film and substrate possesses a columnar structure, and the Ti/a-C:H and (Ti,Ce)/a-C:H carbon-based films are not suffering from any visibly localized delamination, indicating a good adhesion to the substrate. In contrast to the solitary Ti-doped Ti/a-C:H film, the rare earth Ce-modified (Ti,Ce)/a-C:H carbon-based film has a denser and more homogenous structure.

The chemical composition of the as-prepared carbon-based films was measured by XPS at approximately 92.76 at.% C and 1.25 at.% for the Ti/a-C:H film and approximately 93.47 at.% C, 0.96 at.% Ti and 0.28 at.% Ce for the (Ti,Ce)/a-C:H carbon-based film (see Table 2). Moreover, the chemical bonding states of atoms were analyzed using the XPS fine spectrum, as shown in Fig. 3. The Ce 3d XPS spectra in Fig. 3(a) reveal satellite peaks at the binding energies of 904.4 eV and 885.9 eV. Additionally, the $3d_{5/2}$ and $3d_{3/2}$ transitions are located at the binding energies of 882 eV and 900.3 eV, respectively, and the distance between the two transitions is 18.3 eV. These features are consistent with the characteristics of CeO_2.[18–20] The C 1s XPS spectra, as shown in Fig. 3(b), can be deconvoluted into three Gaussian lines centered at 284.5 eV, 285.4 eV and 286.9 eV corresponding to the sp^2-C, sp^3-C, and C–O bonds, respectively. The sp^2-C and sp^3-C peak areas were used to calculate the value of $sp^3/(sp^2+sp^3)$, allowing us to evaluate the relative content of sp^3. The $sp^3/(sp^2+sp^3)$ value is 0.22 for the Ti/a-C:H film and 0.25 for the (Ti,Ce)/a-C:H film.

DLC film is often characterized by Raman spectroscopy. Generally, the Raman spectra of DLC film exhibit an asymmetric broad peak in the range 900–1900 cm^{-1}, which can be deconvoluted into two Gaussian peaks located at around 1560 cm^{-1}(G peak) and 1360 cm^{-1} (D peak).[10,11,24] The G peak position and the intensity ratio of the G peak and D peak (I_D/I_G) reflect the relative content of sp^3-C.[8,10] Figure 4 shows the Raman spectra from 800–2000 cm^{-1} for the as-prepared carbon-based films. It can be seen that the Raman spectra of the Ti/a-C:H film and (Ti,Ce)/a-C:H film exhibit tiny distinctions. The G peak is located at 1547 cm^{-1} for Ti-C:H film and 1545 cm^{-1} for (Ti,Ce)/a-C:H film. The intensity ratios (I_D/I_G) were calculated using the peak areas to be 0.91 and 0.87 for the Ti/a-C:H film and (Ti,Ce)/a-C:H film, respectively, indicating a higher sp^3-C content in the (Ti,Ce)/a-C:H film. Thus, co-doping with a suitable amount of Ce should be beneficial to the formation of sp^3-C.

Table 2. Chemical composition and mechanical properties of Ti/a-C:H and (Ti,Ce)/a-C:H films.

Films	Chemical composition/at.%			Thickness	Hardness	Elastic modulus	H/E	Critical
	C	Ti	Ce	/μm	/GPa	/GPa	ratio	load/N
Ti/a-C:H	92.76	1.25	0	0.89	17.8	136.4	0.13	8
(Ti,Ce)/a-C:H	93.47	0.96	0.28	0.92	19.3	145.8	0.13	22

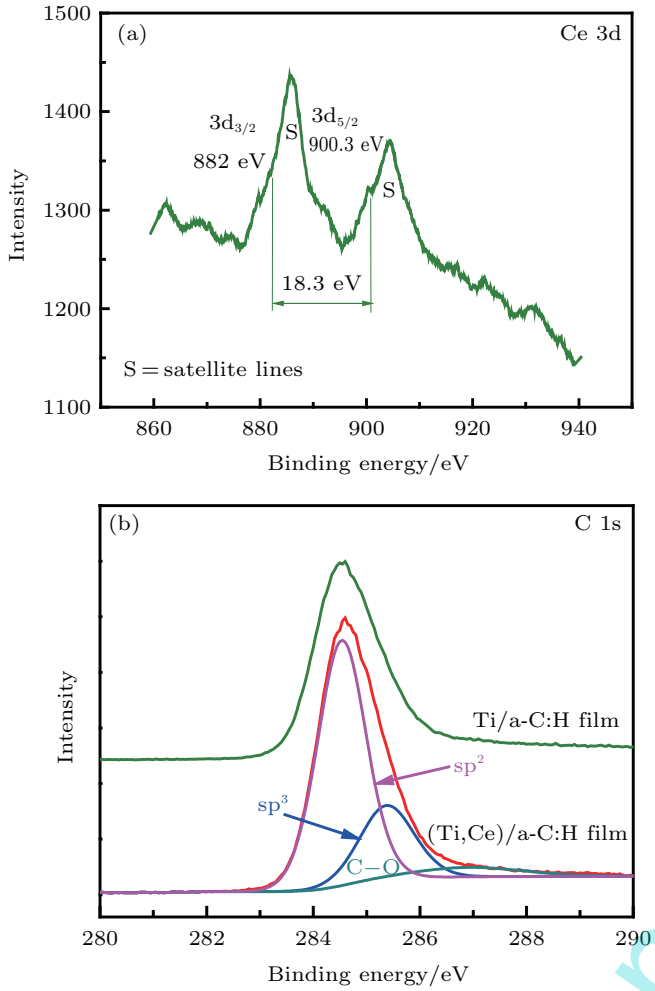

Fig. 3. (color online) XPS (a) Ce 3d spectra of (Ti,Ce)/a-C:H film and (b) C 1s spectra of Ti/a-C:H and (Ti,Ce)/a-C:H films.

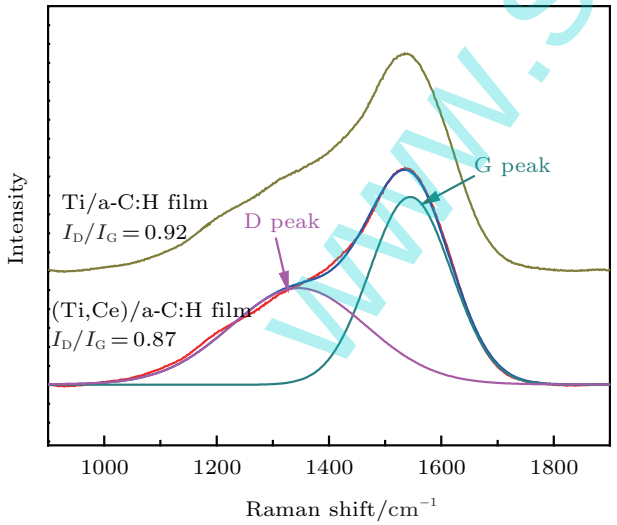

Fig. 4. (color online) Raman spectra of as-prepared Ti/a-C:H film and (Ti,Ce)/a-C:H film.

Figure 5 shows the XRD spectra of the Ti/a-C:H and (Ti,Ce)/a-C:H films. It is clear that both spectra have a TiC peak, whereas there is no information about Ce or CeO_2. The diffraction peak corresponds to the (111) and (200) planes of TiC. In addition, the TiC grains are oriented mainly in the (111) plane for both Ti/a-C:H and (Ti,Ce)/a-C:H carbon-based films. However, the intensity of the TiC(111) diffraction peak has decreased significantly in the Ce co-doped DLC film. Thus, the Ce probably restrains the crystallization of the TiC phase, causing a weak diffraction peak in the TiC phase. There is also a small deviation in the XRD spectra of the two carbon-based films, which can be ascribed to the internal compressive stress.[25] The full-width at half-maximum (FWHM) reflects important information about the crystallinity of the TiC phase.[16] Hence, the FWHM of the (111) peak of the TiC phase was analyzed to investigate the status of the TiC grains in the films. According to Debye–Scherrer's formula,[26] the average crystal size of TiC in the Ti/a-C:H and (Ti,Ce)/a-C:H films is approximately 8 nm.

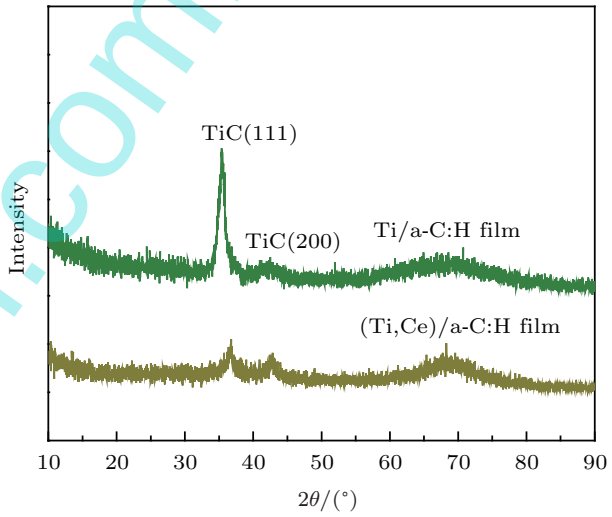

Fig. 5. (color online) XRD spectra of as-prepared Ti/a-C:H and (Ti,Ce)/a-C:H films.

Furthermore, HRTEM was conducted to identify the nanocrystalline and amorphous structures of the as-prepared carbon-based films, as shown in Fig. 6. HRTEM bright-field images reveal that both the Ti/a-C:H and (Ti,Ce)/a-C:H carbon-based films have typical nanocomposite structures in which the nanoparticles (black dots in the images) are uniformly embedded in the amorphous carbon matrix. The corresponding grain sizes in the Ti/a-C:H and (Ti,Ce)/a-C:H carbon-based films are approximately 8 nm. Combined with the previous XPS and XRD analyses, the nanoparticles can be recognized as being in the TiC phase. It has been reported that when the CeO_2 content is $\leq$8 at.%, all the dopant Ce is dissolved within the DLC amorphous matrix as CeO_2.[20] Therefore, the microstructure of the as-prepared rare-earth-modified (Ti,Ce)/a-C:H carbon-based film should mainly consist of TiC nanocrystallites and amorphous carbon as well as dissolved CeO_2.

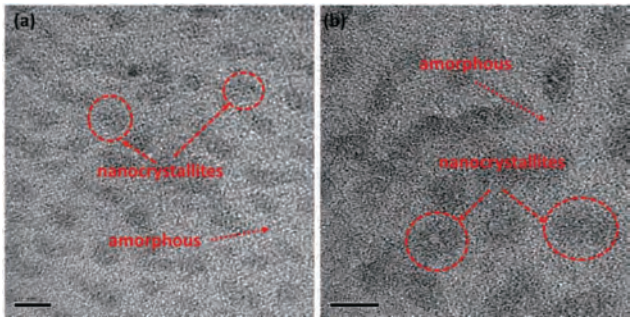

Fig. 6. (color online) HRTEM bright-field images of (a) Ti/a-C:H film and (b) (Ti,Ce)/a-C:H film.

3.2. Mechanical properties

The scratch and nanoindentation technique was used to characterize the mechanical properties of the as-prepared films, and the critical load (L_c) hardness (H), elastic modulus (E), and H/E ratio are presented in Table 2. Obviously, co-doping in DLC could significantly influence the mechanical properties of the as-prepared carbon-based films. The hardness was found to increase, from 17.8 GPa for Ti/a-C:H film to 19.3 GPa for (Ti,Ce)/a-C:H film, as did the elastic modulus (from 136.4 GPa for Ti/a-C:H film to 145.8 GPa for (Ti,Ce)/a-C:H film). From the earlier XPS and Raman analyses, we know there is a relatively higher content of sp^3-C in the (Ti,Ce)/a-C:H film, so it should have a higher hardness than the Ti/a-C:H film. Moreover, as CeO_2 is the main component of glass-polishing materials, the Ce-modified (Ti,Ce)/a-C:H carbon-based film could be expected to have a higher hardness.[27] In particular, both of the as-prepared carbon-based films were measured to have almost the same H/E ratio, indicating that their wear rates should be similar.

The adhesive strength of the Ti/a-C:H and (Ti,Ce)/a-C:H films was evaluated by scratch tests, and the optical microscope images of the scratch tracks are shown in Fig. 7. Note that the Ti/Ce co-doped (Ti,Ce)/a-C:H film has a critical load of 22 N, a significant increase from the 8 N of the solitary Ti/a-C:H film. Notably, the Ti/a-C:H film exhibits more cracks and has the abrupt, localized delamination that is characteristic of severely brittle materials, whereas the (Ti,Ce)/a-C:H film mainly presents plastic deformation and some micro-cracks. As a result, the Ce co-doped film could achieve a much higher adhesive strength than the Ti/a-C:H film. Therefore, the selected rare earth Ce should enhance DLC films to achieve better mechanical properties.

3.3. Friction and wear behavior

Friction tests in ambient air were conducted on the Ti/a-C:H and (Ti,Ce)/a-C:H films. The friction coefficients as a function of sliding time are shown in Fig. 8. It can be seen that the friction coefficients reach stable values of 0.19 for the Ti/a-C:H film and 0.15 for the (Ti,Ce)/a-C:H film. The corresponding wear rates of the Ti/-C:H and (Ti,Ce)/a-C:H films were calculated to be approximately 2.4×10^{-7} mm^3/Nm and 1.3×10^{-7} mm^3/Nm, respectively. The morphologies of the wear tracks and their corresponding wear scars tested in ambient air were characterized by SEM, as shown in Fig. 9. Neither the Ti/a-C:H nor (Ti,Ce)/a-C:H film exhibit serious wear, although the Ti/a-C:H film reveals wider, deeper wear cracks and bigger wear scars.

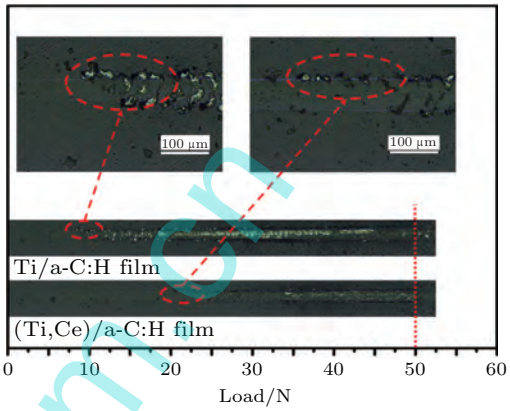

Fig. 7. (color online) The optical microscope images of scratch tracks of the Ti/a-C:H and (Ti,Ce)/a-C:H films.

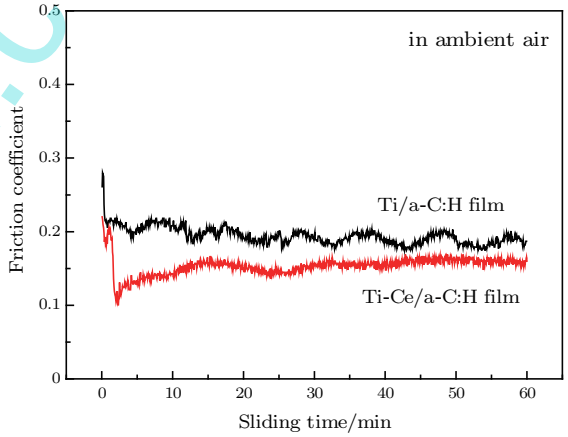

Fig. 8. (color online) Friction coefficient versus sliding time for Ti/a-C:H film and (Ti,Ce)/a-C:H film in ambient air.

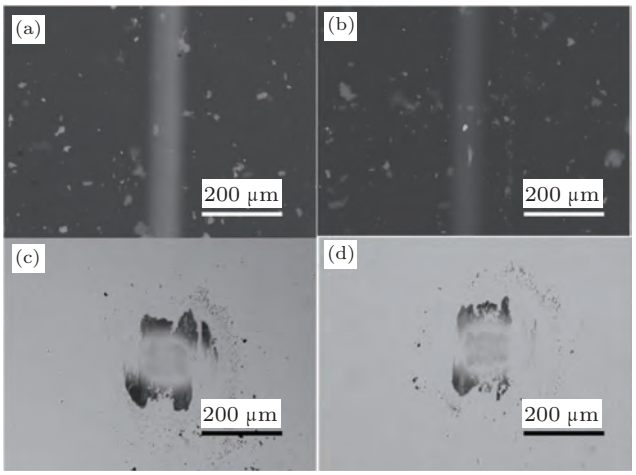

Fig. 9. (color online) SEM images of wear tracks and wear scars on the counterfaces in ambient air for Ti/a-C:H film ((a), (c)) and for (Ti,Ce)/a-C:H film ((b), (d)).

Investigations into the tribological behavior of DLC film confirm that graphitization at the contact area of the ball and the film is the primary reason for low friction.[28,29] The SEM images of the wear scars clearly show a graphitic transferred layer. Moreover, the lower friction coefficient of the (Ti,Ce)/a-C:H film could be a result of the Ce co-doping. It is thought that CeO_2 could accelerate physicochemical reactions at the friction surface and enrich C, O elements in the contact area.[30] Thus, the properties of CeO_2 may favor the formation of a graphitic transferred layer, giving the (Ti,Ce)/a-C:H film a lower friction coefficient. However, the H/E ratio is regarded as the primary material property of DLC film in terms of wear resistance,[31] and the H/E ratios of the Ti/a-C:H film and (Ti,Ce)/a-C:H film are the same. This indicates that the relative content of sp^3-C and hardness might play an important role in the process of friction tests. It has been reported that high hardness prevents wear because of the high carrying capacity under the action of high-speed friction testing.[32,33] From the above XPS, Raman, and mechanical properties analyses, the (Ti,Ce)/a-C:H film possesses a higher relative content of sp^3-C ($sp^3/(sp^2+sp^3) = 0.25$ and $I_D/I_G = 0.83$) and hardness (19.3 GPa), indicating a lower wear rate compared with that of Ti/a-C:H film in ambient air conditions.

The tribological properties of the as-prepared carbon based films were also characterized under deionized water conditions and the friction curves are shown in Fig. 10. The (Ti,Ce)/a-C:H film presents a lower friction coefficient and wear rate in deionized water than the Ti/a-C:H film (friction coefficients of 0.05 and 0.10, respectively, and wear rates of 8.0×10^{-8} mm^3/Nm and 9.2×10^{-8} mm^3/Nm, respectively). The morphologies of the wear tracks and their corresponding wear scars tested under deionized water were characterized by SEM, as shown in Fig. 11. Both films show only slight wear. It can be seen that transfer materials appear at the wear scars of the Ti/a-C:H and (Ti,Ce)/a-C:H films, and there are many granular chips. When testing the friction of the as-deposited hydrogenated carbon-based films in deionized water conditions, a continuous transfer layer could not form on the WC counterface. This is because the hydrogenated structure of the DLC film is vulnerable in water conditions when subjected to sliding wear,[34] as shown in the images of the scars. However, this behavior can be improved by doping elements or using interlayer structures.[34,35] Indeed, the deionized water on the surface of the as-prepared hydrogenated carbon-based films could provide water lubrication and restrain wear. Additionally, a higher hardness and elastic modulus would effectively restrain wear. As a result, the (Ti,Ce)/a-C:H film achieves a lower friction coefficient and suffers less wear.

The friction and wear of the as-prepared carbon based films are different under ambient air and deionized water conditions. Obviously, the friction coefficient and wear rate in ambient air are higher than in deionized water—the friction coefficients went from 0.19 and 0.15 in air to 0.10 and 0.05 in water, and the wear rates decreased from 2.4×10^{-7} m^3/Nm and 1.3×10^{-7} m^3/Nm in air to 9.2×10^{-8} m^3/Nm and 8.0×10^{-8} m^3/Nm in water. This can be attributed to the water lubrication effect resulting in relatively low friction and adhesion, which act to decrease the wear rates of the films. Therefore, this rare earth modified (Ti,Ce)/a-C:H film could feasibly improve the tribological performance of WC cemented carbide in water environments.

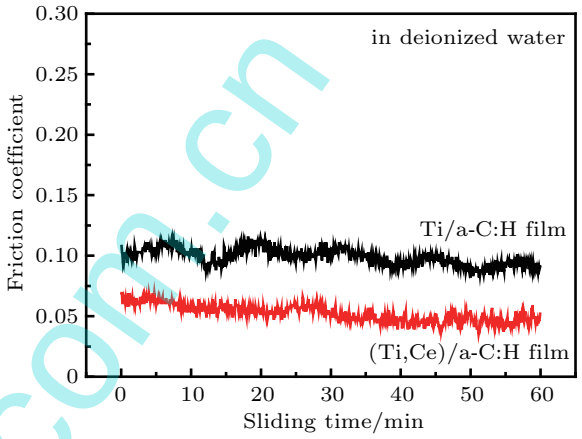

Fig. 10. (color online) Friction coefficient versus sliding time for Ti/a-C:H film and (Ti,Ce)/a-C:H film in deionized water.

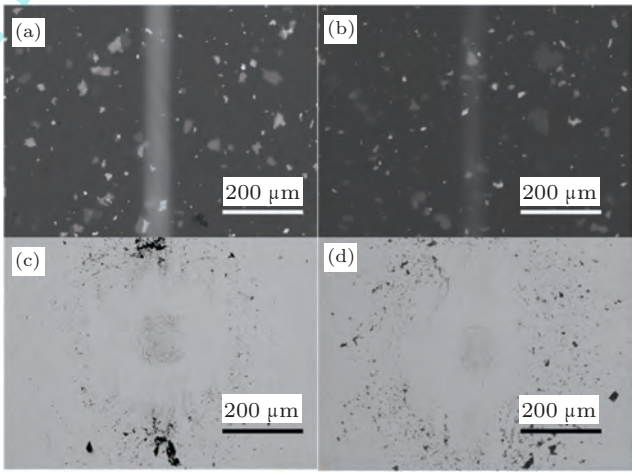

Fig. 11. (color online) SEM images of wear tracks and wear scars on the counterfaces in deionized water for Ti/a-C:H film ((a), (c)) and for (Ti,Ce)/a-C:H film ((b), (d)).

4. Conclusion

A rare earth Ce-modified (Ti,Ce)/a-C:H carbon-based film was successfully deposited on WC cemented carbide using a DC reactive magnetron sputtering process. The morphologies, microstructure, and mechanical properties of the as-prepared film were characterized systematically, and the friction and wear behavior were evaluated in both ambient air and deionized water conditions. Our findings can be summarized as follows:

i) The doping Ti forms TiC nanocrystallites and uniformly disperses in the amorphous carbon matrix, whereas the doping Ce forms CeO_2 that exists with the amorphous phase in the co-doped (Ti,Ce)/a-C:H carbon-based film.

ii) The co-doped (Ti,Ce)/a-C:H carbon-based film exhibits better friction and wear properties compared with the solitary Ti-doped Ti/a-C:H film, achieving a relatively low friction coefficient of 0.15 and wear rate of 1.3×10^{-7} m^3/Nm in ambient air.

iii) The most striking performance was observed in deionized water: the (Ti,Ce)/a-C:H carbon-based film exhibits a lower friction coefficient (0.05) than the Ti/a-C:H film (0.10) and a lower wear rate of 8.0×10^{-8} m^3/Nm, approximately 13.0% less than that of the Ti/a-C:H film. These results indicate that (Ti,Ce)/a-C:H film could feasibly improve the tribological performance of WC cemented carbide in water environments.

References

[1] Li X, Liu Y, Liu B and Zhou J 2016 *Int. J. Refract. Met. Hard Mater.* **56** 132
[2] Su W, Huang Z, Ren X, Chen H and Ruan J 2016 *Int. J. Refract. Met. Hard Mater.* **56** 110
[3] Tarragó J M, Coureaux D, Torres Y, Casellas D, Al-Dawery I, Schneider L and Llanes L 2016 *Mater. Des.* **97** 492
[4] Lauter L, Hochenauer R, Buchegger C, Bohn M and Lengauer W 2016 *J. Alloys Compd.* **675** 407
[5] Vilhena L M, Fernandes C M, Soares E, Sacramento J, Senos A M R and Ramalho A 2016 *Wear* **346-347** 99
[6] Katiyar P K, Singh P K, Singh R and Kumar A L 2016 *Int. J. Refract. Met. Hard Mater.* **54** 27
[7] Beilicke R, Bobach L and Bartel D 2016 *Tribol. Int.* **97** 136
[8] Liu L, Zhou S, Liu Z, Wang Y and Ma L 2016 *Chin. Phys. Lett.* **2** 026801
[9] Kvasnica S, Schalko J, Eisenmenger-Sittner C, Benardi J, Vorlaufer G, Pauschitz A and Roy M 2006 *Diamond Relat. Mater.* **10** 1743
[10] Wang J, Liu G, Wang L, Deng X and Xu J 2008 *Chin. Phys. B* **8** 3108
[11] Zhang Z, Lu X, Luo J, Shao T, Qing T and Zhang C 2006 *Chin. Phys.* **11** 2697
[12] Yang L, Wang Z, Zhang S, Yang L and Chen Q 2009 *Chin. Phys. B* **12** 5401
[13] Jiang J, Wang Y, Wang Q, Huang H, Wei Z and Hao J 2016 *Chin. Phys. B* **4** 048101
[14] Wang Q, Zhou F, Zhou Z, Yang Y, Yan C, Wang C, Zhang W, Li L K Y, Bello I and Lee S T 2012 *Diamond Relat. Mater.* **25** 163
[15] Cui J, Qiang L, Zhang B, Ling X, Yang T and Zhang J 2012 *Appl. Surf. Sci.* **12** 5025
[16] Zhou S, Wang L, Wang S C and Xue Q 2011 *Appl. Surf. Sci.* **15** 6971
[17] Jao J Y, Han S, Chang L S, Chen Y, Chang C and Shih H C 2009 *Diamond Relat. Mater.* **2** 368
[18] Zhang Z, Zhou H, Guo D, Gao H and Kang R 2008 *Appl. Surf. Sci.* **5** 2655
[19] Zhang Z, Jia Z, Wang Y, Wang F and Yang R 2008 *Surf. Coat. Technol.* **24** 5947
[20] Zhang Z, Lu X, Guo D, Xu J and Luo J 2008 *Diamond Relat. Mater.* **3** 396
[21] Pauschitz A, Kvasnica S, Jisa R, Bernardi J, Koch T and Roy M 2008 *Diamond Relat. Mater.* **12** 2010
[22] Zhang Z, Lu X, Luo J, Liu Y and Zhang C 2007 *Diamond Relat. Mater.* **11** 1905
[23] Zhang Z, Zhou H, Guo D, Wu D and Tong Y 2009 J. *Alloys Compd.* **1** 318
[24] Zhang D, Shen B and Sun F 2010 *Appl. Surf. Sci.* **8** 2479
[25] Zhang S, Xie H, Zeng X and Hing P 1999 *Surf. Coat. Technol.* **2** 219
[26] Zdujić M V, Milošević O B and Karanović L Č 1992 *Mater. Lett.* **13** 125
[27] He L, Su Y, Lanhong J and Shi S 2015 *J. Rare Earths* **8** 791
[28] Liu Y, Erdemir A and Meletis E I 1996 *Surf. Coat. Technol.* **82** 48
[29] Singh V, Jiang J C and Meletis E I 2005 *Thin Solid Films* **1** 150
[30] Du P, Chen G, Song S, Chen H, Li J and Shao Y 2016 *Tribol. Lett.* **62** 29
[31] Leyland A and Matthews A 2000 *Wear* **1** 1
[32] Charitidis C A 2010 *Int. J. Refract. Met. Hard Mater.* **1** 51
[33] Modabberasl A, Kameli P, Ranjbar M, Salamati H and Ashiri R 2015 *Carbon* **94** 485
[34] Ronkainen H, Varjus S and Holmberg K 2001 *Wear* **3** 267
[35] Ronkainen H, Varjus S and Holmberg K 1998 *Wear* **2** 120